

Effect of orifice diameter, depth of air injection, and air flow rate on oxygen transfer in a pilot-scale, full lift, hypolimnetic aerator¹

K.I. Ashley, D.S. Mavinic, and K.J. Hall

Abstract: A pilot-scale, full lift, hypolimnetic aerator was used to examine the effect of diffuser pore diameter, depth of diffuser submergence, and gas flow rate on oxygen transfer, using four standard units of measure for quantifying oxygen transfer: (a) K_{La20} (h^{-1}), the oxygen transfer coefficient at 20 °C; (b) SOTR ($\text{g O}_2\text{-h}^{-1}$), the standard oxygen transfer rate; (c) SAE ($\text{g O}_2\text{-kWh}^{-1}$), the standard aeration efficiency and (d) SOTE (%), the standard oxygen transfer efficiency. Diffuser depth (1.5 and 2.9 m) exerted a significant effect on K_{La20} , SOTR, SAE, and SOTE, with all units of measure increasing in response to increased diffuser depth. Both K_{La20} and SOTR responded positively to increased gas flow rates (10, 20, 30, and 40 $\text{L}\cdot\text{min}^{-1}$), whereas both SAE and SOTE responded negatively. Orifice diameter (140, 400, and 800 μm) exerted a significant effect on K_{La20} , SOTR, SAE, and SOTE, with all units of measure increasing with decreasing orifice size. These experiments demonstrate how competing design factors interact to determine overall oxygen transfer rates in full lift hypolimnetic aeration systems. The practical application for full lift hypolimnetic aerator design is to maximize the surface area of the bubbles, use fine (i.e., $\sim 140 \mu\text{m}$) pore diameter diffusers, and locate the diffusers at the maximum practical depth.

Key words: hypolimnetic aeration, lake restoration, oxygen transfer, re-aeration.

Résumé : Un aérateur hypolimnique à levée complète construit à l'échelle pilote a été utilisé pour étudier l'effet du diamètre des pores du diffuseur, de la profondeur de submersion du diffuseur et du débit de gaz sur le transfert d'oxygène. L'aérateur utilise quatre unités standard de mesure afin de quantifier le transfert d'oxygène : (a) le coefficient de transfert d'oxygène à 20 °C, K_{La20} (h^{-1}); (b) le taux de transfert d'oxygène standard (SOTR) ($\text{g O}_2\text{-h}^{-1}$); (c) l'efficacité d'aération standard (SAE) ($\text{g O}_2\text{-kWh}^{-1}$) et (d) l'efficacité du transfert d'oxygène standard (SOTE) (%). La profondeur du diffuseur (1,5 m et 2,9 m) avait un impact important sur le K_{La20} , le SOTR, la SAE et la SOTE, et la réponse de toutes les unités de mesure augmentait avec l'augmentation de la profondeur du diffuseur. Le K_{La20} et le SOTR ont répondu de manière positive à l'augmentation des débits de gaz (10, 20, 30 et 40 $\text{L}\cdot\text{min}^{-1}$), alors que la SAE et la SOTE ont répondu de manière négative. Le diamètre des orifices (140, 400 et 800 μm) avait un impact important sur le K_{La20} , le SOTR, la SAE et la SOTE, la réponse de toutes les unités de mesure augmentait avec la diminution de la dimension des orifices. Ces expériences démontrent l'interaction entre les facteurs de conception pour déterminer les taux de transfert global de l'oxygène dans les systèmes d'aération hypolimniques à levée complète. L'utilisation pratique de cette conception d'aérateur hypolimnique à levée complète est de maximiser la surface active des bulles, d'utiliser des diffuseurs avec un diamètre de pores fin (c.-à-d. $\sim 140 \mu\text{m}$) et de localiser les diffuseurs à la profondeur maximale pratique.

Mots-clés : aération hypolimnique, restauration des lacs, transfert d'oxygène, réaération.

[Traduit par la Rédaction]

Introduction

Hypolimnetic aeration has developed into an important water quality improvement technique, due to its ability to selectively increase oxygen concentrations in the hypolimnion of stratified lakes and reservoirs in situ, while maintaining thermal stratification. However, after nearly 50 years of

extensive testing and reporting, hypolimnetic aeration is infrequently used by civil engineers to improve potable water quality in eutrophic lakes and reservoirs. This seems paradoxical in light of evolving regulatory requirements for higher quality raw water supplies and the well documented capabilities of hypolimnetic aeration for improving water quality (see Lorenzen and Fast 1977, for review). The au-

Received 28 October 2007. Revision accepted 10 October 2008. Published on the NRC Research Press Web site at cjce.nrc.ca on 19 December 2008.

K.I. Ashley,² D.S. Mavinic, and K.J. Hall.³ Environmental Engineering Group, Department of Civil Engineering, 2324 Main Mall, University of British Columbia, Vancouver, BC V6T 1W5, Canada.

Written discussion of this article is welcomed and will be received by the Editor until 31 May 2009.

¹A paper submitted to the Journal of Environmental Engineering and Science.

²Corresponding author (e-mail: ken.ashley@shaw.ca).

³Present address: 1957 Westview Drive, North Vancouver, BC V7M 3B1, Canada.

thors believe this situation is largely a result of the interdisciplinary nature of hypolimnetic aeration, where most of the research and reporting has been conducted by limnologists and fisheries biologists. The conservative tendency for many civil engineers has been to address raw water quality concerns through conventional water treatment facilities, rather than accept risks with less predictable “ecological engineering” approaches in lakes or reservoirs. However, with increasingly stringent regulations for permissible concentrations of disinfection by-products (e.g., trihalomethanes and haloacetic acids) eliminating such traditional practices as chlorine pre-treatment, it is inevitable that water utilities will be forced to adopt more pro-active watershed, lake and reservoir management strategies for their raw water supplies. This can be achieved through strict control of watershed land use, implementing rainwater “best management practices”, and by using in-lake techniques such as hypolimnetic aeration to improve and (or) maintain higher quality raw water.

Since hypolimnetic aeration is one of the most effective in-lake water quality improvement techniques, it is necessary to provide updated design information to water treatment engineers, so that hypolimnetic aeration can be integrated into current and future water quality management strategies. Fast and Lorenzen (1976) and Fast et al. (1976) provided a comparative analysis of various hypolimnetic aerator designs in the mid 1970s; however, experimental verification of design factors capable of influencing the oxygen transfer efficiency of full lift hypolimnetic aerators has been lacking. McGinnis and Little (2002) and Burris et al. (2002) have developed predictive models of oxygen transfer and water flow rates in hypolimnetic aerators, and these models can be used to compare field measurements with their model’s predictions. Given the increasing cost and greenhouse gas implications of fossil fuel derived electricity, it is imperative that oxygen transfer efficiency is factored into any potential in-lake water quality improvement strategy, since the cumulative operational and maintenance costs of numerous large electric pumps and air compressor motors can be substantial. For example, on the North American continent, the aeration of wastewater consumes between 50 and 90% of the total energy costs of a typical municipal treatment facility, with annual aeration operating costs of 0.6 billion in 1982 US dollars (ASCE 1988).

Accordingly, this study conducted a detailed comparative analysis of three design factors that influence the oxygen transfer capabilities of a full lift hypolimnetic aerator, which is a design used throughout North America, Western Europe, and Japan. The experiments utilized nonsteady-state gas transfer methodology in a pilot-scale system. Specifically, the research examined the effect of diffuser pore diameter, depth of diffuser submergence and gas flow rate on oxygen transfer using four standard units of measure for quantifying oxygen transfer: (a) $K_L a_{20}$ (h^{-1}), the oxygen transfer coefficient at 20 °C; (b) SOTR ($\text{g O}_2 \cdot \text{h}^{-1}$), the standard oxygen transfer rate; (c) SAE ($\text{g O}_2 \cdot \text{kWh}^{-1}$), the standard aeration efficiency, and (d) SOTE (%), the standard oxygen transfer efficiency. The purpose of this research was to determine which combination(s) of design factors was most effective at dissolving oxygen into water, under laboratory test conditions, of a pilot-scale, full lift hypolimnetic aerator.

Methods

Full lift hypolimnetic aerator and tank dimensions

The pilot-scale, full lift hypolimnetic aerator was based on a modified Bernhardt (1974) design, as described in Ashley (1988). The unit was constructed of clear acrylic, and consisted of an open separator box (82 cm (l) \times 36 cm (w) \times 28 cm (h) outside dimensions) fitted with 282.2 cm inlet and outlet tubes (19.5 cm inside diameter) (Fig. 1). The tube entrance and exit were at 90°, as there was insufficient space in the aeration tank to attach a tapered intake flare or discharge elbow. The aeration tank was filled to a depth of 3.1 m for the tests; hence the operational volume was 1194 L. The tank was built with two panels (300 cm \times 30 cm \times 25.4 mm) of clear acrylic to allow viewing of the tank interior and the aerator (Fig. 2).

Tank mixing, velocity measurement, and probe locations

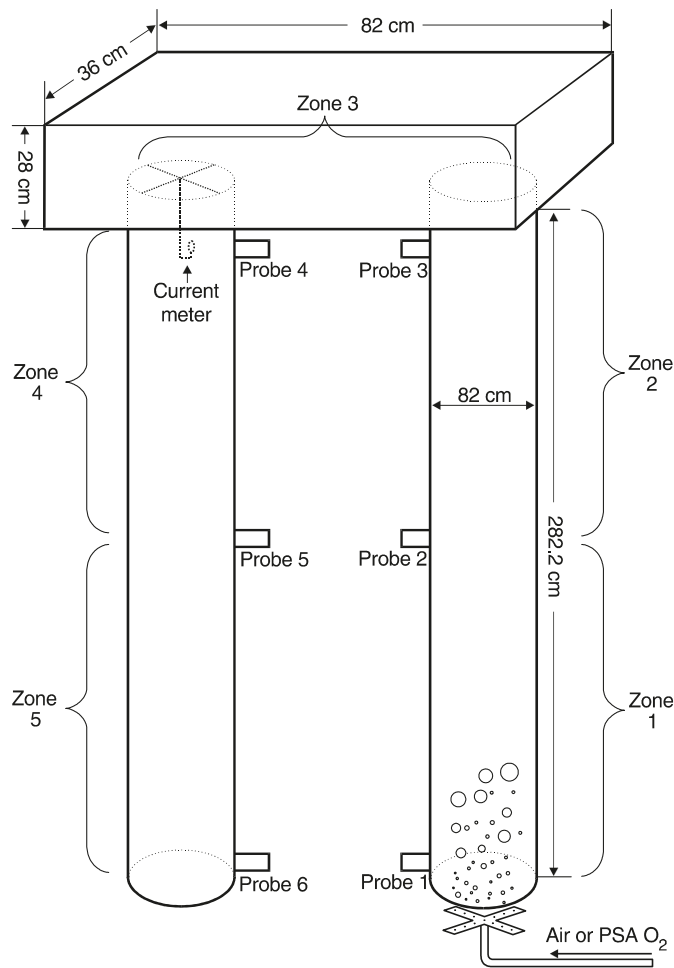
An acrylic divider (200 cm (h) \times 38 cm (w)) was inserted into the tank between the inlet and outlet tubes, and extended from the tank bottom to beneath the separator box, thereby prevent short-circuiting of oxygenated water from the outlet tube immediately back into the inlet tube. The divider rested on the tank floor, so the two tubes were effectively separated for a vertical distance of 200 cm, leaving 110.5 cm for water exchange over the top of the divider. Dye tests indicated the divider sheet was an effective barrier to short circuiting (Ashley 2002). Two submersible mixing pumps (4500 $\text{L} \cdot \text{h}^{-1}$ each) were located in diagonal corners on the tank floor, to ensure complete mixing of the deoxygenation chemicals without using the aerator. Dye tests and oxygen probe readings confirmed that the tank was rapidly mixed with both pumps operating (maximum pumping rate = 9000 $\text{L} \cdot \text{h}^{-1}$), since the oxygen saturation throughout the tank was reduced to <1% saturation (within an average of 2 min) following the addition of a sodium sulfite solution.

A velocity sensor was suspended on a wire frame in the centre of the downflow tube, 28 cm from the junction with the floor of the separator box (Fig. 1). The inlet and outlet tubes were fitted with oxygen probe insertion ports near both ends of the tubes, and at the mid-point of each tube. The oxygen probes were arranged in the tank to ensure that the tank was completely mixed, to validate the nonsteady-state re-aeration test (ASCE 1992). The probes were numbered according to their position in the aerator as follows (Fig. 1): Probe 1 was located 8 cm from the inlet of the inflow tube, operating at a depth of 283 cm; Probe 2 was located at the midpoint of the inflow tube, operating at a depth of 150 cm; Probe 3 was located 8 cm from the outlet of the inflow tube, operating at a depth of 17 cm; Probe 4 was located 8 cm from the inlet of the outflow tube, operating at a depth of 17 cm; Probe 5 was located at the midpoint of the outflow tube, operating at a depth of 150 cm, and Probe 6 was located 8 cm from the outlet of the outflow tube, operating at a depth of 283 cm. Probe 7 was the % oxygen by volume probe, used to track the purity of the oxygen content of the introduced air and Probe 8 was a temperature probe located at the 3.0 m level.

Water, compressed air, and oxygen supply

The water used in the tests was from the UBC water supply, which is low in total dissolved solids (22 $\text{mg} \cdot \text{L}^{-1}$). A

Fig. 1. Schematic of full lift aerator with several probe locations shown.

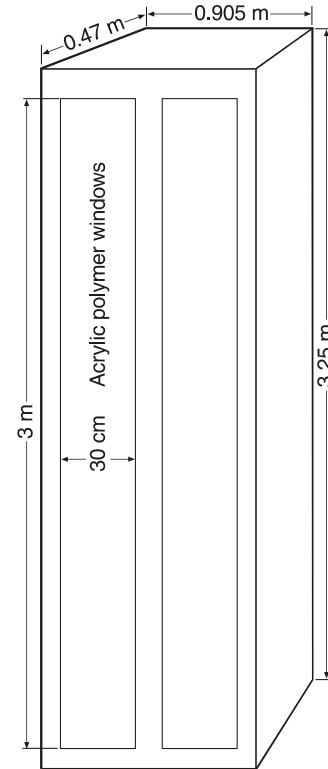


44.74 kW Quincy rotary screw compressor (Model QNW 260-D), rated at 6800 L·min⁻¹ (240 standard cubic feet per minute; SCFM) supplied the compressed air for the building. A nominal efficiency filter and water-cooled aftercooler was fitted to the discharge end of the compressor. Oxygen gas for the experiments was produced by an AS-20 oxygen generator (AirSep Corporation, Buffalo, New York), and stored in a 227 L receiver. The purity of oxygen generated ranged from 90 to 95%. A reference cylinder of certified oxygen gas (>99.99% oxygen), obtained from Air Liquide Canada, was used to calibrate the oxygen gas probe (i.e., Probe 7) and continuously monitor the purity of the AirSep oxygen.

Instrumentation, parameter measurement, and data logging

A manifold board (Point Four Systems Inc., Coquitlam, BC) distributed and regulated the air flow and delivery pressure. Inflowing compressed air, from the laboratory supply, passed through a Wilkerson 5.0 μm particulate and oil–water filter, then a 0.01 μm particulate filter and oil–water filter. The filtered air was then routed via separate regulators to an array of three mechanical flow indicators, which could be operated independently, or in any combination. The coarse-scale flow meter was a Brooks Sho-rate flow indica-

Fig. 2. Schematic diagram of aeration tank.



tor, with 150 mm scale, 2 to 46 L·min⁻¹; the medium scale meter was a Brooks Sho-rate flow indicator with 150 mm scale, 2 to 12 L·min⁻¹; and the fine scale meter was a Key Instruments flow indicator with 80 mm scale, 0 to 3.5 L·min⁻¹, all calibrated for 100% oxygen. The Brooks flow indicators were designed to operate at 3.2 bar (45 psig) (1 bar = 100 kPa), and the Key Instruments flow indicator was designed for 3.5 bar (50 psig), although it was operated at 3.2 kg bar.

Flow meter readings were corrected by a specific density correction factor (i.e., $\sqrt{1.105/1.0}$) when operated on compressed air. The Key Instruments meter was corrected by a pressure correction factor (i.e., $\sqrt{59.7/64.7}$) to compensate for the lower operating pressure (i.e., 3.2 vs. 3.5 bar). All of the flow meters were calibrated for 21 °C; hence, no temperature correction factor was required. The air supply for the % volume probe cup (i.e., Probe 7) was located downstream of the three flow indicators; however, the volumetric flow rate of air to the probe cup was so low that it did not introduce a bias to the various flow meter readings. The air exiting the probe cup was vented into an 11 cm water filled cylinder, so that the air flow could be directly observed in a bubble stream and adjusted to maintain a low, but constant discharge rate. Water velocity was measured by a Marsh McBirney Model 2000 flow meter, using a fixed point averaging (FPA) program to dampen the output variation. A duration of 120 s was used for the averaging period.

A PT4 Monitor (Point Four Systems Inc., Coquitlam, BC) was supplied with seven OxyGuard probes (OxyGuard International, Denmark), which are membrane-covered, self-polarizing, galvanic measuring elements, with a built-in

temperature compensation. The Oxyguard probes were configured to measure dissolved oxygen in percent (i.e., %) saturation, rather than $\text{mg}\cdot\text{L}^{-1}$, as the % saturation probe membranes were 50% thinner than the $\text{mg}\cdot\text{L}^{-1}$ membranes, resulting in a faster probe response time. Water temperature was measured with a dedicated stainless steel thermister probe (Channel 8) on the PT4 Monitor, and a secondary temperature probe on the YSI meter. Both probes were typically within ~ 0.2 °C, and the PT4 temperature reading was used for the probe calibration procedure. The PT4 temperature probe was checked in an ice bath (0 °C) and room temperature (20 °C) water, as determined by a mercury calibration thermometer, and found to be accurate within 0.5 °C. An eight-channel, microprocessor based PT4 Monitor (Point Four Systems Inc., Coquitlam, BC) was used to record and log data collected during the experiments. The unit was configured with 6 channels for measuring percent dissolved oxygen saturation in water (Ch. 1–6), one percent (by volume) oxygen channel (Ch. 7) for measuring the oxygen content of the incoming gas and one water temperature channel (Ch. 8). Continuous visual checks were made during each test to ensure the upstream gas pressure remained constant at 3.2 kg bar, and that gas flow remained at the desired delivery rate.

Experimental design

The design variables examined were the effect of diffuser orifice pore diameter (140, 400, and 800 μm), effect of diffuser depth (1.5 and 2.9 m), and effect of air flow rate (10, 20, 30, and 40 $\text{L}\cdot\text{min}^{-1}$). An additional treatment examined the feasibility of downflow bubble contact aeration (DBCA) type of flow pattern in the outlet tube. In this test (Misc. Test 1), the aeration system was operated with only the tank mixing pumps to circulate the water, without any airlift in the inlet tube. A small amount of air was introduced via a 2 μm ultra-fine bubble diffuser in the separator box, so the tiny bubbles generated by the diffuser were swept downwards into the outlet tube in a quasi-DBCA mode.

This resulted in four possible combinations of gas flow rate for each category of diffuser depth and orifice diameter (Table 1). Each of the combinations was completed, then repeated in a different randomly selected order, to remove any random error that may have occurred during any given treatment day. Each of the main treatments were replicated 3 times, the minimum number of replicates recommended for non-steady state re-aeration tests (ASCE 1992). A total of 75 individual re-aeration tests were completed (Table 2).

Test procedure, oxygen calibration, and oxygenation protocol

The basic test procedure started with filling the tank with tap water, turning on the submersible mixing pumps and allowing the tank water to circulate for 5–6 min. Replicate samples of water were then collected from 10 cm below the tank surface in 300 mL BOD bottles, and analyzed for dissolved oxygen, using the Winkler titration procedure (Azide modification; Lind 1979). The two Winkler readings were then averaged to provide the reference oxygen concentration to calibrate the PT4 unit and oxygen probes for the day. The percent saturation for dissolved oxygen on each test day was calculated according to eq. [1] in Colt (1984):

$$[1] \quad C_s^* = C_s^*760(\text{BP} - P_{\text{H}_2\text{O}})/(760.0 - P_{\text{H}_2\text{O}})$$

where C_s^* is the the dissolved oxygen air-solubility value ($\text{mg}\cdot\text{L}^{-1}$) for the ambient barometric pressure, temperature and vapor pressure of water; C_s^*760 is the dissolved oxygen air-solubility value ($\text{mg}\cdot\text{L}^{-1}$) for the barometric pressure equal to 760.0 mm Hg and ambient temperature; BP is the barometric pressure in mm Hg; $P_{\text{H}_2\text{O}}$ is the vapor pressure of water in mm Hg for the ambient temperature.

Values for C_s^*760 and $P_{\text{H}_2\text{O}}$ were taken from reference tables in Colt (1984), and the barometric pressure for each test day was taken from the Vancouver weather station on the Environment Canada WebPage (at www.weatheroffice.com).

The percent oxygen saturation of the test water was then determined using eq. [2], on each day:

$$[2] \quad \frac{(\text{Winkler 1 (mg L}^{-1}) + \text{Winkler 2 (mg L}^{-1})) / 2}{C_s^* (\text{mg L}^{-1})} \times 100 = \% \text{ oxygen saturation}$$

The PT4 Monitor was then calibrated with this value, using the single point calibration procedure outlined in the PT4 software (Point Four Systems 1997). The probe response was examined from 0% saturation (sulfite bath) to 100% saturation (AirLiquide certified >99.99% oxygen gas) and found to be essentially linear; hence, this calibration procedure was satisfactory. Once calibrated, the probes were quite stable, but were still re-calibrated each test day. The oxygen concentration in air (% volume) was monitored by a dedicated probe (Ch 7), in the PT4 Monitor. This probe was calibrated daily using a reference cylinder of certified oxygen gas (>99.99% oxygen). The probe was then calibrated to this reference standard, using the same single point calibration procedure.

The deoxygenation–oxygenation procedure used was the nonsteady-state re-aeration test (ASCE 1992; Boyd and Watten 1989). Water in the tank was deoxygenated with 0.1 $\text{mg}\cdot\text{L}^{-1}$ of cobalt chloride (certified grade of $\text{CoCl}_2\cdot 6\text{H}_2\text{O}$) and 10.0 $\text{mg}\cdot\text{L}^{-1}$ of sodium sulfite (Sulftech Catalyzed Na_2SO_3 ; Code 098-3393) for each 1.0 $\text{mg}\cdot\text{L}^{-1}$ of dissolved oxygen present in the water (Boyd 1986); an additional 10% weight of Na_2SO_3 was added, to ensure rapid deoxygenation at the colder test temperatures. Mixing details can be found elsewhere (Ashley 2002). The YSI meter and PT4 monitor confirmed that the tank water was rapidly deoxygenated, as the % oxygen saturation invariably declined to <1.0% within 2 min. Water in the tank was allowed to mix for 6 min before re-aeration treatments were initiated.

Each experimental test was terminated when the % saturation recorded at Probe 1 (i.e., the intake to the inlet tube, see Fig. 1) reached 60% saturation. This represented the % oxygen saturation of the bulk water in the test tank at the end of the test run. The % saturation reading of the remaining probes within the full lift aerator were typically greater than 60% saturation, as they were subject to the discharge of the experimental combination being tested, which raised the % saturation above the ambient % saturation in the bulk tank water. A maximum of six test runs were conducted on each tank of water, before draining and refilling, to ensure that the total dissolved solids concentration did not exceed 2000 $\text{mg}\cdot\text{L}^{-1}$ as recommended by ASCE (1992).

Table 1. List of treatments for full lift hypolimnetic aeration experiments.

Test No.	Gas flow (L·min ⁻¹)	Orifice diameter (μm)	Depth (m)	Gas composition	Options
1	10, 20, 30, 40	140	2.9	air	n/a
2	10, 20, 30, 40	140	1.5	air	n/a
3	10, 20, 30, 40	400	2.9	air	n/a
4	10, 20, 30, 40	400	1.5	air	n/a
5	10, 20, 30, 40	800	2.9	air	n/a
6	10, 20, 30, 40	800	1.5	air	n/a
Misc. 1	3	2	0	air	Pump only/DBCA

Table 2. List of treatment combinations for the full lift hypolimnetic aeration experiments.

Test No.	No. of combinations	Replicates	Total number of tests
1	4	3	12
2	4	3	12
3	4	3	12
4	4	3	12
5	4	3	12
6	4	3	12
		Sub-total	72
Misc. 1	1	3	3
		Sub-total	3
		Total	75

Parameter estimation procedure

The log deficit method of parameter estimation was used to determine $K_L a$, the oxygen transfer coefficient (h^{-1}), since the experimental tests were terminated at 60% saturation, due to the time impracticality of running all tests to 98% of saturation (as is mandatory for the nonlinear regression method of parameter estimation (ASCE 1992)). The nonlinear method is the recommended American Society of Civil Engineers (ASCE) method of parameter estimation for the measurement of oxygen transfer in clean water; “however, if the engineer/owner so specifies, the log deficit method described in Annex E shall be permitted in lieu of the nonlinear regression method.” (ASCE 1992). The log deficit method is also the recommended technique for parameter estimation within the aquacultural and aquatic sciences community (Boyd 1986; Boyd and Watten 1989) and was listed as a tentative standard in the 15th Edition of Standard Methods (APHA 1980). Details of $K_L a$ determination can be found elsewhere (Ashley 2002).

K_{LaT} was corrected to K_{La20} according to eq. [3] (ASCE 1992):

$$[3] \quad K_{La20} = K_{LaT} \theta^{(20-T)}$$

where T is test water temperature in °C; $\theta = 1.024$.

SOTR was calculated as

$$[4] \quad \text{SOTR} = K_{La20} C_{s20} V$$

where SOTR is the standard oxygen transfer rate ($\text{g O}_2 \cdot \text{h}^{-1}$); K_{La20} is the oxygen transfer coefficient at 20 °C (h^{-1}); C_{s20} = dissolved oxygen concentration ($\text{mg} \cdot \text{L}^{-1}$) at saturation for 20 °C and standard pressure (760 mm Hg); V is the volume of water in the tank (m^3).

Standard aeration efficiency (SAE) was calculated as

$$[5] \quad \text{SAE} = \text{SOTR}/\text{power input}$$

where SAE is the standard aeration efficiency ($\text{g O}_2 \cdot \text{kWh}^{-1}$); SOTR is the standard oxygen transfer rate ($\text{g O}_2 \cdot \text{h}^{-1}$); power input (kW) is the total delivered power (kW).

Details of power input calculations are presented elsewhere (Ashley 2002).

Finally, SOTE was calculated as

$$[6] \quad \text{SOTE} = \text{SOTR}/W_{\text{O}_2}$$

where SOTE is standard oxygen transfer efficiency (%); SOTR is standard oxygen transfer rate ($\text{g O}_2 \cdot \text{h}^{-1}$); W_{O_2} is mass flow rate of oxygen in the gas flow stream ($\text{g O}_2 \cdot \text{h}^{-1}$).

The detailed calculation of W_{O_2} , for the various experimental treatments, can be found elsewhere (Ashley 2002).

Statistical analysis

The statistical model used to analyze the experimental data was the general linear model (i.e., GLM) in the SYSTAT 10 statistical package (Systat Software Inc., Chicago, IL). This model can estimate any univariate or multivariate general linear model, including analysis of variance or covariance (Wilkinson and Coward 2000). The level of significance was set at $\alpha = 0.01$ for each statistical test, rather than the traditional $\alpha = 0.05$, to conclusively demonstrate highly significant treatment effects. The approach used in the statistical analysis was to analyze individual groups of experiments that were designed to test for a particular treatment effect (e.g., effect of depth of gas release and effect of orifice diameter) as a function of gas flow rate (as the covariate). This resulted in a basic analysis of covariance with first order interactions (e.g., depth by gas flow rate). An initial analysis of covariance model was then used to determine if there was any significant interaction between the covariate (i.e., gas flow rate) and the experimental treatments (orifice diameter and depth of air release). In these experiments, interaction is defined as treatment combinations where the observed effect was greater than that predicted by the sum of the treatments. For example, if the K_{La20} at 40 $\text{L} \cdot \text{min}^{-1}$ was more than twice that at 20 $\text{L} \cdot \text{min}^{-1}$, it would indicate an interaction effect of that particular combination of gas flow rate and orifice diameter. Scheffé's Test ($\alpha = 0.01$) was used to test for significance, in the comparison among treatment means. Scheffé's test is designed to allow all possible linear combinations of group means to be tested. The result is that Scheffé's test is more conservative than other tests, and a larger difference is required to obtain a significant re-

sult (Wilkinson and Coward 2000). Scheffé's test is the most rigorous a posteriori test, and is recommended by statistical purists for comparison among means tests (Larkin 1975).

Results

Results for this study are presented, collectively, in Tables 3–7 and Figs. 3–5. A significant depth treatment effect, and a flow rate covariate effect ($\alpha \leq 0.01$) was obtained for the 140 μm diffuser (Figs. 3a–3d). $K_L a_{20}$, SOTR, SAE, and SOTE increased in value with an increase in depth of gas release. A significant depth by flow rate interaction effect was observed for $K_L a_{20}$ and SOTR (Table 3), indicating the treatment depth effect was significantly influenced by the air flow rate. The significant depth by flow rate interaction effect indicates that $K_L a_{20}$ and SOTR increased 1.5 fold at the 2.9 m diffuser depth, with increasing gas flow rate, as compared to the 1.5 m diffuser depth (Figs. 3a–3b). SAE and SOTE were not influenced by the depth by flow rate interaction effect (as shown by the near parallel slopes), and declined with increasing gas flow rate. The mean SAE and SOTE at 2.9 m was 323.8 g O₂-kWh⁻¹ and 7.9%, a 43% and 52% increase over the mean SAE of 227.2 g O₂-kWh⁻¹ and SOTE of 5.2% recorded at 1.5 m (Figs. 3c–3d and Table 3).

The analysis of covariance for the 400 μm diffuser produced equally significant results ($\alpha \leq 0.01$) for the depth treatment, and flow rate covariate effect for $K_L a_{20}$, SOTR, SAE, and SOTE (Figs. 4a–4d). All parameters increased in value with depth of gas release. A significant depth by flow rate interaction effect was observed for $K_L a_{20}$ and SOTR (Table 4). The significant depth by flow rate interaction effect indicates that $K_L a_{20}$ and SOTR increased 1.4 fold at the 2.9 m diffuser depth with increasing gas flow rate, as compared to the 1.5 m diffuser depth (Figs. 4a–4b). SAE and SOTE were not influenced by the depth by flow rate interaction effect, and declined with increasing gas flow rate. The mean SAE and SOTE at 2.9 m was 237.8 g O₂-kWh⁻¹ and 5.8%, a 32% and 41% increase over the mean SAE of 179.6 g O₂-kWh⁻¹ and SOTE of 4.1% recorded at 1.5 m (Figs. 4c–4d and Table 4).

The 800 μm diffuser also exhibited a significant effect ($\alpha \leq 0.01$) for the depth treatment and flow rate covariate effect for $K_L a_{20}$, SOTR, SAE, and SOTE (Figs. 5a–5d), with all parameters increasing in value with depth of gas release. A significant depth by flow rate interaction effect was again observed for $K_L a_{20}$ and SOTR (Table 5). The significant depth by flow rate interaction effect indicates that $K_L a_{20}$ and SOTR increased 1.5 fold at the 2.9 m diffuser depth with increasing gas flow rate, as compared to the 1.5 m diffuser depth (Figs. 5a–5b). As observed with the 140 μm and 400 μm diffusers, SAE and SOTE did not demonstrate a depth by flow rate interaction effect, and declined with increasing gas flow rate. The mean SAE and SOTE at 2.9 m was 197.1 g O₂-kWh⁻¹ and 4.8%, a 41% and 50% increase over the mean SAE of 139.9 g O₂-kWh⁻¹ and SOTE of 3.2% recorded at 1.5 m (Figs. 5c–5d and Table 5).

The results of the full lift tests, in quasi-DBCA mode, were considerably different from the regular performance of the full lift hypolimnetic aerator. The mean values for $K_L a_{20}$, SOTR, and SAE were among the lowest recorded for any of the full lift tests; however, the mean SOTE values were the

highest recorded (Table 6). The low values of $K_L a_{20}$ and SOTR (Table 7) were related to the low gas flow rate (i.e., 3 L·min⁻¹) used in these experiments, which were ~1/3 of the gas flow rates used in the lowest gas flow setting for the full lift tests (i.e., 10 L·min⁻¹).

Discussion

Diffuser depth

Diffuser depth exerted a significant effect on $K_L a_{20}$, SOTR, SAE, and SOTE, with all units of measure showing positive responses to increased diffuser submergence. The magnitude of the responses were all quite large, ranging from 30 to 57% (Tables 3–5). The depth of gas release influenced $K_L a_{20}$, SOTR, and SOTE, mainly by an increase in bubble contact time due to the longer path length the bubbles must take to reach the surface, and a larger deficit or driving force ($C_i - C_L$); this resulted in more oxygen transfer (Mavinic and Bewtra 1974, 1976). The increase in SAE was unexpected, as similar studies with an upward, co-current, air-water flow observed a decrease in SAE with increased diffuser submergence (i.e., System II; Mavinic and Bewtra 1976).

The SAE increased in these experiments, as there was an increase in the bubble-travel distance, an increase in driving force ($C_i - C_L$), as well as an increase in water velocity, which increased turbulence at the liquid interface, and influenced K_L . Water velocity data (Ashley 2002) demonstrated that velocity increased with diffuser depth, in each experimental treatment combination, thus supporting this conclusion. The fact that SAE increased with diffuser submergence, in this case, indicates that, despite the additional air power energy required to deliver air to greater depths, the energy cost was more than offset by the increased oxygen transfer resulting from the longer bubble contact times, greater turbulence and increased hydrostatic pressure. Unlike the Mavinic and Bewtra (1976) study, there were no energy requirements for pumping water in this system, which was a significant energy demand in their Systems II, III, and IV. In addition, the outlet tube water from the full lift aerator discharged into the bulk liquid in the tank, hence inlet tube water rise velocities increased with diffuser submergence, but not to the same extent as the circulating, closed-loop system design of Mavinic and Bewtra (1976). This resulted in greater initial turbulence in the inlet tube where the diffuser was located, as tank water entering the inlet tube had little velocity; hence, high shear forces were present as the rising air bubbles mixed with the slower moving water entering the inlet tube from the bulk liquid reservoir.

Gas flow rate

Gas flow rate significantly influenced $K_L a_{20}$, SOTR, SAE, and SOTE in all of the experimental combinations. $K_L a_{20}$ and SOTR responded positively to increased gas flow rates, a response noted in numerous gas transfer studies (e.g., Bewtra et al. 1970; Schmit et al. 1978). At least two mechanisms are responsible for this effect. Firstly, higher gas flow rates generate increased turbulence at the liquid interface. Under highly turbulent conditions, mass transfer is regulated by the disruption and rate of renewal of the liquid film, as

Table 3. Adjusted least squares means (\pm SE), treatment and interaction effects for the 140 μm diffuser on air at 1.5 m and 2.9 m depth.

Treatment	K_{La20} (h^{-1})	SOTR ($\text{g O}_2\cdot\text{h}^{-1}$)	SAE ($\text{g O}_2\cdot\text{kWh}^{-1}$)	SOTE (%)	n
1.5 m	2.1 (0.09)	23.2 (0.95)	227.2 (7.39)	5.2 (0.18)	12
2.9 m	3.3 (0.09)	35.7 (0.95)	323.8 (7.39)	7.9 (0.18)	12
Interaction	Yes, 1.52	Yes, 1.52	No	No	
Depth	sig, $p = 0.000$	sig, $p = 0.000$	sig, $p = 0.000$	sig, $p = 0.000$	
Flow rate	sig, $p = 0.000$	sig, $p = 0.000$	sig, $p = 0.000$	sig, $p = 0.000$	

Table 4. Adjusted least squares means (\pm SE), treatment and interaction effects for the 400 μm diffuser on air at 1.5 m and 2.9 m depth.

Treatment	K_{La20} (h^{-1})	SOTR ($\text{g O}_2\cdot\text{h}^{-1}$)	SAE ($\text{g O}_2\cdot\text{kWh}^{-1}$)	SOTE (%)	n
1.5 m	1.7 (0.04)	18.1 (0.44)	179.6 (5.9)	4.1 (0.14)	12
2.9 m	2.3 (0.04)	25.5 (0.44)	237.8 (5.9)	5.8 (0.14)	12
Interaction	Yes, 1.40	Yes, 1.40	No	No	
Depth	sig, $p = 0.000$	sig, $p = 0.000$	sig, $p = 0.000$	sig, $p = 0.000$	
Flow rate	sig, $p = 0.000$	sig, $p = 0.000$	sig, $p = 0.000$	sig, $p = 0.000$	

Table 5. Adjusted least squares means (\pm SE), treatment and interaction effects for the 800 μm diffuser on air at 1.5 m and 2.9 m depth.

Treatment	K_{La20} (h^{-1})	SOTR ($\text{g O}_2\cdot\text{h}^{-1}$)	SAE ($\text{g O}_2\cdot\text{kWh}^{-1}$)	SOTE (%)	n
1.5 m	1.3 (0.02)	14.5 (0.21)	139.9 (2.86)	3.2 (0.07)	12
2.9 m	2.0 (0.02)	22.1 (0.21)	197.1 (2.86)	4.8 (0.07)	12
Interaction	Yes, 1.50	Yes, 1.50	No	No	
Depth	sig, $p = 0.000$	sig, $p = 0.000$	sig, $p = 0.000$	sig, $p = 0.000$	
Flow rate	sig, $p = 0.000$	sig, $p = 0.000$	sig, $p = 0.000$	sig, $p = 0.000$	

Table 6. Mean (\pm SE) K_{La20} , SOTR, SAE, and SOTE values for full lift hypolimnetic aerator operating in pump only DBCA mode on air at 3 $\text{L}\cdot\text{min}^{-1}$.

Treatment	K_{La20} (h^{-1})	SOTR ($\text{g O}_2\cdot\text{h}^{-1}$)	SAE ($\text{g O}_2\cdot\text{kWh}^{-1}$)	SOTE (%)	n
Pump only- air	0.6 (0.01)	6.2 (0.14)	8.0 (0.18)	11.3 (0.25)	3

Table 7. Hypothetical comparison of pump only, Group 7 and Group 1 values.

Parameter	Pump only value	Pump only \times 3.3	Group 1:10 L min^{-1}
K_{La20} Air (h^{-1})	0.6	2.0	1.5
SOTR Air ($\text{g O}_2\cdot\text{h}^{-1}$)	6.2	20.7	16.0
SAE Air ($\text{g O}_2\cdot\text{kWh}^{-1}$)	8.0	26.7	349.4

described by the Danckwartz surface rejuvenation theory, in eq. [7] (Dobbins 1964):

$$[7] \quad K_L = \sqrt{D_L r}$$

where K_L is a liquid film coefficient ($\text{m}\cdot\text{h}^{-1}$); D_L is the diffusion coefficient for oxygen ($\text{m}^2\cdot\text{h}^{-1}$); r is the rate of renewal of liquid film (h^{-1}).

As r increases, K_L increases. Therefore, one mechanism by which higher gas flow rates increase K_{La20} and SOTR is via their positive effect on K_L . Secondly, increased gas flow rates increase the number of bubbles present in the water column per unit time. This increases the total interfacial area available for gas transfer to the surrounding medium

(Bewtra and Mavinic 1978). Therefore, increased gas flow rates also positively influence K_{La20} and SOTR by their effect on “ a ”.

SAE and SOTE responded negatively to increased gas flow rates, which is a common observation in diffused aeration systems (Bewtra and Nicholas 1964; Ellis and Stansbury 1980; Mavinic and Bewtra 1976). The accepted explanation for this response is that air bubbles become larger with an increase in gas flow rates. This results in less oxygen transfer, due to the reduced ratio of interfacial area to bubble volume. Secondly, as air bubbles become larger, their terminal rise velocities increase, thus reducing the contact time between air bubbles and the surrounding liquid, even though there is a corresponding velocity induced increase in turbu-

Fig. 3. Effect of diffuser depth on (a) K_La_{20} , (b) SOTR, (c) SAE, and (d) SOTE; diffuser pore diameter of 140 μm .

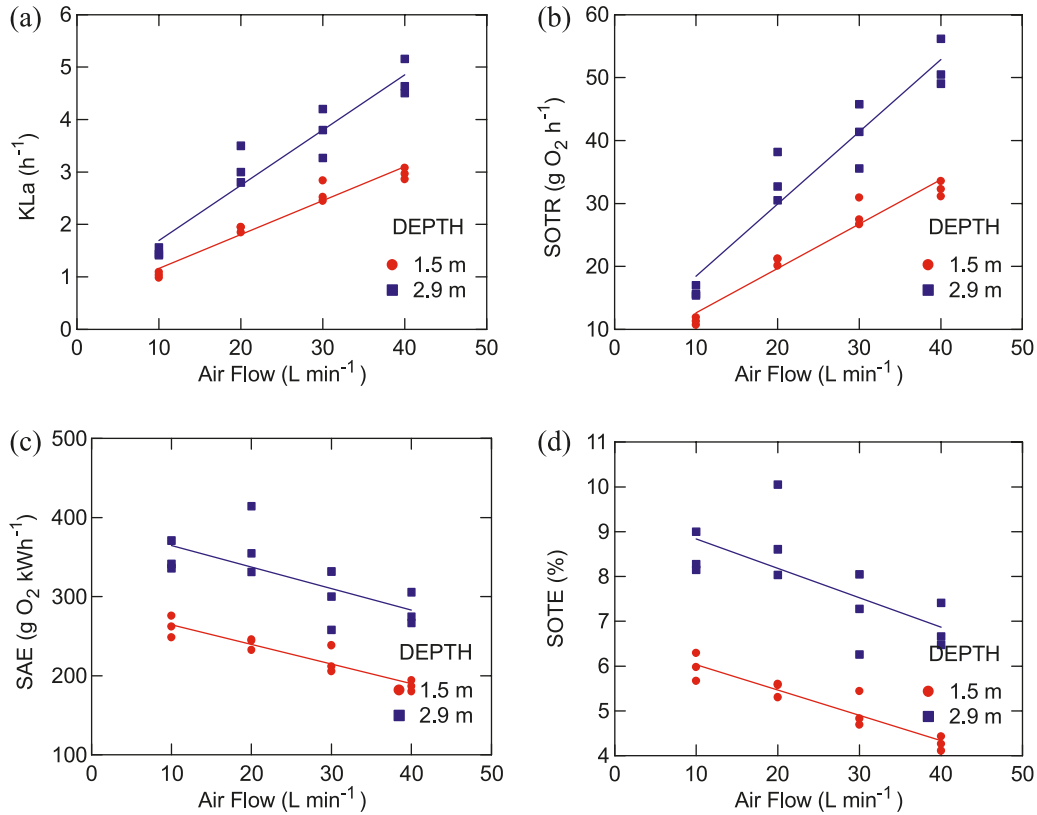


Fig. 4. Effect of diffuser depth on (a) K_La_{20} , (b) SOTR, (c) SAE, and (d) SOTE; diffuser pore diameter of 400 μm .

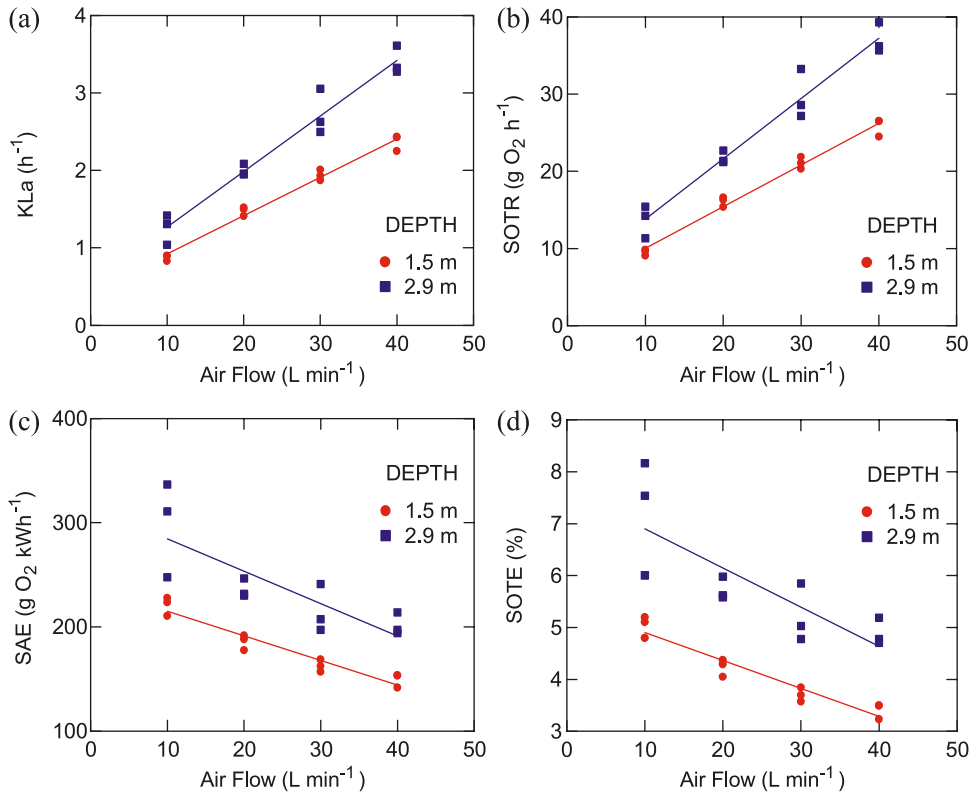
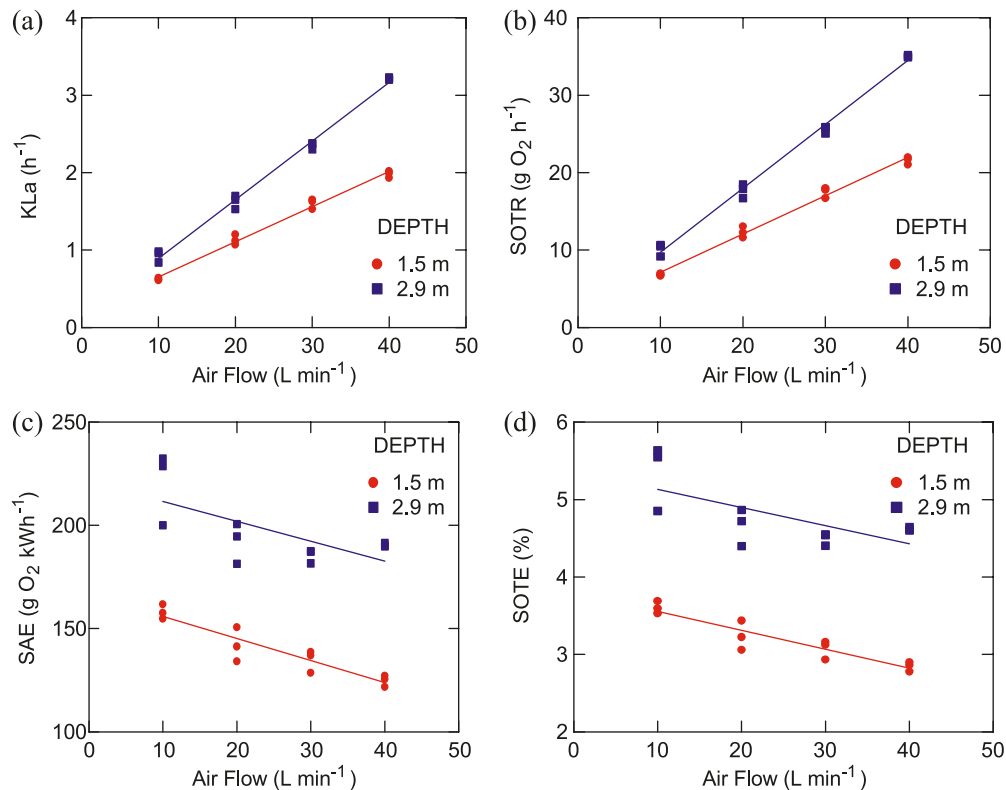


Fig. 5. Effect of diffuser depth on (a) $K_L a_{20}$, (b) SOTR, (c) SAE, and (d) SOTE; diffuser pore diameter of 800 μm .



lence at the liquid film. Finally, increased gas flow rates incur additional energy costs for gas compression, which penalises SAE. This is a classic example of how competing factors interact to determine overall oxygen transfer rates.

Orifice diameter

Orifice diameter exerted a significant effect on $K_L a_{20}$, SOTR, SAE, and SOTE. Each unit of measure increased with decreasing orifice size (Tables 3–5). Smaller orifices produce smaller bubbles, and a reduction in bubble size influences gas transfer in at least four ways: smaller bubbles have (a) a greater surface area per unit bubble volume (Eckenfelder 1969), (b) a decrease in terminal rise velocity (Stenstrom and Gilbert 1981), (c) a decrease in the liquid film coefficient (Bewtra and Nicholas 1964), and (d) an increase in the total number of bubbles in the water column per unit gas discharge.

An increase in bubble surface area per unit volume increases the “a” in $K_L a$, and acts to increase $K_L a_{20}$ and SOTR. A decrease in terminal rise velocity increases the bubble contact time, which acts to increase $K_L a_{20}$, SOTR, SOTE, and SAE, since no additional energy costs are incurred. However, the competing response is that a decrease in terminal rise velocity decreases the liquid film coefficient (K_L) and turbulence at the liquid interface, which decreases $K_L a_{20}$, SOTR, SAE, and SOTE. Increased numbers of bubbles in the water column, per unit time, increases the surface area available for gas transfer. However, if the bubbles are in a confined column, they can exert the opposite effect by saturating the interstitial water between the bubbles, thus re-

ducing the oxygen concentration gradient across the liquid film (Mavinic and Bewtra 1974).

The interaction of these opposing factors determines the net effect on $K_L a_{20}$, SOTR, SAE, and SOTE. In these experiments, the overall effect of smaller bubbles was an increase in all units of measure, indicating that the effect of increased surface area and contact time more than compensated for the reduction in K_L due to slower rise velocities and increased bubble density in the inlet tube. Since the reduction in orifice diameters did not require an increase in energy, SAE responded positively for the same reasons. If orifice diameter were reduced below a critical minimum diameter (e.g., <2 μm), then additional energy would be required to force gas through such an ultra-fine pore diffuser and overcome surface tension at the orifice–water interface, and SAE would likely decline accordingly. The diffusers used in the DBCA experiments were in the 2 μm size range, and required considerable back pressure before any gas could be seen emerging from the diffuser. In contrast, the 140, 400, and 800 μm diffusers had minimal backpressure, and responded instantly to fluctuations in gas flow rate.

A number of researchers have reported a similar effect of increased SOTE, with decreased bubble diameter. For example, Morgan and Bewtra (1960) and Bewtra and Nicholas (1964) both observed increased SOTE with fine bubble (Saran tubes) as compared to coarse bubble diffusers (Spargers). Barnhardt (1969) also demonstrated a decrease in $K_L a_{20}$ with bubble diameters of 2 mm and larger.

The comparison among means test (i.e., Scheffé’s) indicated that each orifice size was significantly different from

each other, for the four units of measure. Since Scheffé's test is conservative by design and the most rigorous a posteriori test for performing comparison among means (Larkin 1975), there is little doubt the observed results were real, and not statistical artifacts.

Pump only DCBA mode

The pump only, full lift tests in DCBA mode were conducted as curiosity driven research, to determine if there was any advantage to operating a full lift hypolimnetic aerator using circulating water pumps as the prime mover of the system, rather than air lift pumps. Interestingly, if one multiplies the $K_L a_{20}$, SOTR, and SAE values from the Pump Only tests by 3.3 (i.e., $10 \text{ L}\cdot\text{min}^{-1}/3 \text{ L}\cdot\text{min}^{-1}$) to standardize the gas flow rates, the hypothetical results, for $K_L a_{20}$ and SOTR on air, appear more efficient per unit of gas flow than the values from the Group 1 tests (Table 7). However, when one considers the SAE comparison in Table 7, the hypothetical pump only SAE values on air were only ~7–8% of those recorded during the Group 1 tests. The pump only DCBA mode gas flow rate was limited to $3 \text{ L}\cdot\text{min}^{-1}$ due to the design capacity of the ultra-fine pore (i.e., $2 \mu\text{m}$ dia.) diffuser, hence a direct comparison with the full lift test results (i.e., $10 \text{ L}\cdot\text{min}^{-1}$) was not possible.

The explanation for this discrepancy is that the actual SAE values obtained during the Group 1 tests, on air, used considerably less energy to compress and deliver the air, than was required to operate the circulating pumps in the hypothetical standardized Pump Only SAE comparison. This hypothetical comparison, and the fact that the SOTE values recorded during the pump only tests were quite high (i.e., 11.3%), indicate that a pump only configuration *may* be a reasonable option if one wished to design a system that is high in SOTE, at the expense of reduced SAE performance. This could be an appropriate application of this technology in situations where energy costs were negligible, and the objective was to simply increase oxygen concentrations in the hypolimnion. In certain cases, where dissolution of Fe^{+2} and Mn^{+2} from bottom sediments was problematic, a highly efficient design with lower mass loading of oxygen could be used simply to maintain a positive oxidation–reduction potential in hypolimnion, without maintaining elevated dissolved oxygen concentrations. This type of response was observed in Medical Lake, Wash., where an undersized hypolimnetic aeration system was responsible for a significant improvement in hypolimnetic water quality, despite an absence of free dissolved oxygen (Soltero et al. 1994). To increase the SAE performance of this DCBA design configuration, the outlet tube should be extended to take advantage of increased hydrostatic pressure and the resulting improvements in gas transfer. The conceptual origins of the downflow air injection aeration system, as described in the aeration literature (Lorenzen and Fast 1977), may have originated from similar observations.

Summary and conclusions

These experiments illustrated a number of key aspects of gas transfer relevant to full lift hypolimnetic aerator design. Increased depth of submergence and decreased orifice diameter, within the ranges explored in these tests, were design

variables that were beneficial to all units of measure. This demonstrated the importance of contact time, gas partial pressure gradient, and increased interfacial bubble area on oxygen transfer. The effect of increasing gas flow rate was similar across all depths and orifice diameters, clearly demonstrating the overriding importance of higher turbulence and interfacial areas for increasing $K_L a_{20}$ and SOTR, and the negative implications on SAE and SOTE arising from greater energy costs of air delivery. The practical application for full lift hypolimnetic aerator design is to maximize the surface area of the bubbles, use fine (i.e., $\sim 140 \mu\text{m}$) pore diameter diffusers, and locate the diffusers at the maximum practical depth. A balancing act between optimizing $K_L a$ and SOTR, and SAE and SOTE is readily apparent. The designers of hypolimnetic aeration systems will often be presented with the scenario of enhancing some aspects of gas transfer, while sacrificing others, to achieve the desired oxygenation goals. The findings of this study should prove useful to water treatment engineers designing full lift hypolimnetic aeration systems as part of an overall in-lake water quality improvement strategy.

Acknowledgements

The authors wish to acknowledge the financial support provided by NSERC (Natural Sciences and Engineering Research Council of Canada), as well as the technical assistance provided by the staff in the Environmental Lab and Civil Engineering workshop, at UBC. The authors are also grateful to Dr. Richard Speece, of Vanderbilt University, Nashville Tenn., for providing a critical review of this work.

References

- APHA. 1980. Standard methods for the examination of water and wastewater. 15th ed. American Public Health Association, American Water Works Association and Water Pollution Control Federation, Wash.
- ASCE. 1988. Aeration. Manual of Practice FD-13. American Society of Civil Engineers, 601 Wythe St., Alexandria, Va. ISBN 0-87262-673-3.
- ASCE. 1992. Measurement of oxygen transfer in clean water. ANSI/SSCE 2-91. 2nd ed., June 1992. American Society of Civil Engineers, New York.
- Ashley, K.I. 1988. Hypolimnetic aeration research in British Columbia. Verh. Internat. Verein. Limnol. **23**: 215–219.
- Ashley, K.I. 2002. Comparative analysis of oxygen transfer in full lift and Downflow Bubble Contact hypolimnetic aerators. Ph.D. thesis, Civil Engineering Dept., University of British Columbia, BC. 298 pp.
- Barnhardt, E.L. 1969. Transfer of oxygen in aqueous solutions. J. Sanit. Eng. Div. Proc. ASCE, **95**(SA3): 645–661.
- Bewtra, J.K., and Nicholas, W.R. 1964. Oxygenation from diffused air in aeration tanks. J. Water Pollut. Control Fed. **36**: 1195–1224.
- Bewtra, J.K., Nicholas, R.W., and Polkowski, L.B. 1970. Effect of temperature on oxygen transfer in water. Water Res. **4**: 115–122. doi:10.1016/0043-1354(70)90023-0.
- Bewtra, J.K., and Mavinic, D.S. 1978. Diffused aeration systems from theory to design. Can. J. Civ. Eng. **5**: 32–41.
- Boyd, C.E. 1986. A method for testing aerators for fish tanks. Prog. Fish-Cult. **48**: 68–70. doi:10.1577/1548-8640(1986)48<68:AMFTAF>2.0.CO;2.
- Boyd, C.E., and Watten, B.J. 1989. Aeration systems in aquaculture. Rev. Aquat. Sci. **1**: 425–472.

- Burris, V.L., McGinnis, D.F., and Little, J.C. 2002. Predicting oxygen transfer and water flow rate in airlift aerators. *Water Res.* **36**: 4605–4615. doi:10.1016/S0043-1354(02)00176-8. PMID:12418663.
- Colt, J. 1984. Computation of dissolved gas concentrations in water as functions of temperature, salinity and pressure. American Fisheries Society Special Publication No. 14. Bethesda, Md.
- Dobbins, W.E. 1964. Mechanisms of gas absorption by turbulent liquids. *In* Advances in Water Research Proceedings of the 1st International Conf. Water Pollution Research. Pergamon Press Ltd., London, England. Vol. 2, p. 61.
- Eckenfelder, W.W. (Editor). 1969. Oxygen transfer and aeration. *In* Manual of Treatment Processes. Vol. 1. Environmental Sciences Services Corp.
- Ellis, S.E., and Stansbury, R. 1980. The scale-up of aerators. *In* Symposium on The Profitable Aeration of Waste Water, London, April 1980. Paper No. 3. BHRA Fluid Engineering, Cranfield, Bedford. UK.
- Fast, A.W., and Lorenzen, M.W. 1976. Synoptic survey of hypolimnetic aeration. *J. Environ. Eng. Div. Proc. ASCE*, **106**(EE6): 1161–1173.
- Fast, A.W., Lorenzen, M.W., and Glenn, J.H. 1976. Comparative study with costs of hypolimnetic aeration. *J. Environ. Eng. Div. Proc. ASCE*, **106**(EE6): 1175–1187.
- Larkin, P.A. 1975. Biometrics. Biology 300 Course Book, Fall Term, 1975. University of British Columbia, BC. 206 p.
- Lind, O.T. 1979. Handbook of Common Methods in Limnology. 2nd ed. Edited by C.V. Mosby. St. Louis, Mo 199 p.
- Lorenzen, M., and Fast, A.W. 1977. A guide to Aeration/Circulation techniques for lake management. EPA-600/3-77-004. U. S. Environmental Protection Agency.
- Mavinic, D.S., and Bewtra, J.K. 1974. Mass transfer of oxygen in diffused aeration systems. *Can. J. Civ. Eng.* **1**: 71–84.
- Mavinic, D.S., and Bewtra, J.K. 1976. Efficiency of diffused aeration systems in wastewater treatment. *J. Water Pollut. Control Fed.* **48**: 2273–2283.
- McGinnis, D.F., and Little, J.C. 2002. Predicting diffused bubble oxygen transfer rate using the discrete-bubble model. *Water Res.* **36**: 4627–4635. doi:10.1016/S0043-1354(02)00175-6. PMID:12418665.
- Morgan, P.F., and Bewtra, J.K. 1960. Air diffuser efficiencies. *J. Water Pollut. Control Fed.* **32**: 1047–1059.
- Point Four Systems. 1997. PT4 Users Manual. UBC Civil Engineering, Dept. Point Four Systems, Inc., Richmond, BC.
- Schmit, F.L., Wren, J.D., and Redmon, D.T. 1978. The effect of tank dimensions and diffuser placement on oxygen transfer. *J. Water Pollut. Control Fed.* **50**: 1750–1767.
- Soltero, R.A., Sexton, L.M., Ashley, K.I., and McKee, K.O. 1994. Partial and full lift hypolimnetic aeration of Medical Lake, WA to improve water quality. *Water Res.* **28**: 2297–2308. doi:10.1016/0043-1354(94)90045-0.
- Stenstrom, M.K., and Gilbert, R.G. 1981. Effects of alpha, beta and theta factor upon the design, specification and operation of aeration systems. *Water Res.* **15**: 643–654. doi:10.1016/0043-1354(81)90156-1.
- Wilkinson, L., and Coward, M. 2000. Linear models II: Analysis of variance. Chapter 15 in SYSTAT 10, Statistics 1. SPSS Inc., Chicago, Ill.

List of symbols

- α (alpha) statistical level of significance
- BP barometric pressure (mm Hg)
- C_1 dissolved oxygen concentration at time t_1 (mg·L⁻¹)
- C_2 dissolved oxygen concentration at time t_2 (mg·L⁻¹)
- C_s^* dissolved oxygen air-solubility value (mg·L⁻¹) for the ambient barometric pressure, temperature and vapor pressure of water
- C_s^{*760} dissolved oxygen air-solubility value (mg·L⁻¹) for the barometric pressure equal to 760.0 mm Hg and ambient temperature
- C_{s20} dissolved oxygen concentration in water (mg·L⁻¹) at 20 °C and for the barometric pressure of 760.0 mm Hg
- ID inside diameter (cm)
- $K_L a$ overall oxygen transfer coefficient (h⁻¹)
- $K_L a_{20}$ oxygen transfer coefficient at 20 °C (h⁻¹)
- $K_L a_T$ oxygen transfer coefficient at temperature T (h⁻¹)
- P_{H2O} vapor pressure of water for the ambient temperature (mm Hg)
- r^2 coefficient of determination
- SAE standard aeration efficiency (g O₂·kWh⁻¹)
- SOTE standard oxygen transfer efficiency (%)
- SOTR standard oxygen transfer rate (g O₂·h⁻¹)
- θ (theta) = 1.024
- V volume of the liquid (m³)
- W_{O2} mass flow rate of oxygen in the gas flow stream (g O₂·h⁻¹)